Translational Oncology
www.transonc.com

Volume 1 Number 4 December 2008 pp. 187–194 187

Diffusion Magnetic Resonance Imaging: An Imaging Treatment Response Biomarker to Chemoradiotherapy in a Mouse Model of Squamous Cell Cancer of the Head and Neck[1]

Daniel A. Hamstra*, Kuei C. Lee†, Bradford A. Moffat†, Thomas L. Chenevert†, Alnawaz Rehemtulla*,† and Brian D. Ross†

*Department of Radiation Oncology, The University of Michigan Medical School, Biomedical Sciences Research Building, Room A528, Ann Arbor, MI 48109-2200, USA; †Department of Radiology, The University of Michigan Medical School, Biomedical Sciences Research Building, Room A528, Ann Arbor, MI 48109-2200, USA

Abstract

For the treatment of squamous cell cancer of the head and neck (SCCHN), the assessment of treatment response is traditionally accomplished by volumetric measurements and has been suggested to be prognostic for an eventual response to treatment. An early evaluation response during the course of radiation therapy could provide an opportunity to tailor treatment to individual patients. Diffusion magnetic resonance imaging (MRI) allows for the quantification of tissue water diffusion values, thus treatment-induced loss of tumor cells will result in the increase in water mobility at the microscopic level, which can be detected as an increase in tumor diffusion values before any volumetric changes occur. We evaluated the use of diffusion MRI as an imaging biomarker of treatment response in an orthotopic mouse model of SCCHN. Mice with murine squamous cells expressing the yeast transgene cytosine deaminase were treated with 5-fluorocytosine (5FC), ionizing radiation, and combined therapy and were compared with control animals both during and after treatment for changes in tumor volumes, diffusion values, and survival. Radiation therapy had minimal effect on volumetric growth rate, diffusion, or survival. Although 5FC and combination treatment resulted in similar reductions in tumor volumes, the combination treatment elicited a much greater increase in tumor diffusion values, which correlated with improved survival. Thus, diffusion MRI as an imaging biomarker has a potential for early evaluation of the response to chemoradiation treatment in SCCHN.

Translational Oncology (2008) 1, 187–194

Introduction

There will be an estimated 47,000 cancers of the mouth, tongue, pharynx, and larynx in the United States in 2008 with approximately 11,000 deaths [1]. As such, squamous cell cancer of the head and neck (SCCHN) will makeup 2.5% of all cancers and 1% of all deaths caused by cancer during this period. Greater than 90% of these cases are composed of the common histologic diagnosis, squamous cell carcinoma. Surgery remains the mainstay of treatment in head and neck cancer; however, more than 60% of all SCCHN are present in a locally advanced stage where surgery alone is no longer considered curative. Therefore, the combination of chemotherapy and radiation therapy either adjuvantly after maximal surgical resection or as definitive treatment has become the standard of care for many patients [2].

Chemotherapy alone has an excellent response rate in SCCHN with up to 80% overall response and complete response (CR) rates

Address all correspondence to: Daniel A. Hamstra, MD, PhD, University of Michigan, Center for Molecular Imaging, 109 Zina Pitcher Place, Ann Arbor, MI 48109-2200.
E-mail: dhamm@umich.edu

[1]D.A.H. was supported by an ASCO Foundation Young Investigator Award. Support was also provided by a National Institutes of Health grant (P50CA01014).
Received 11 August 2008; Revised 19 September 2008; Accepted 22 September 2008

DOI 10.1593/tlo.08166

in the range of 25% when using multiagent induction chemotherapy [3]. However, despite these excellent response rates, there is little evidence for a survival benefit with induction chemotherapy followed by either surgery or definitive radiation therapy, although a recent meta-analysis did reveal a small survival benefit to induction chemotherapy before radiotherapy [4]. In contrast, the addition of concurrent chemotherapy to radiation therapy (most typically platinum based chemotherapy) has proven to provide a significant benefit in terms of local control and overall survival in both definitive and adjuvant radiation therapies in the treatment of locally advanced SCCHN [2–4].

Typically, evaluation of response to therapy in head and neck cancer has been through physical examination, evaluation in the operating suite through direct laryngoscopy, and by cross-sectional imaging [computed tomography (CT) or magnetic resonance imaging (MRI)] [3]. An early evaluation of tumor response may provide prognostic information about treatment efficacy and allow subsequent tailoring of interventions based upon individual response such as using image-guided adaptive radiotherapy [5]. Computed tomography has been evaluated as a noninvasive means for evaluating the response of induction chemoradiotherapy before surgical resection for SCCHN. However, in this case, strictly volumetric response based on CT examinations gave both poor positive and negative predictive values when compared to histologic finding obtained at resection [6]. Computed tomographic examinations have also been used to evaluate response to radiation therapy both during treatment and 8 to 10 weeks after the completion of treatment [7–11]. Some authors have suggested that rapid response during radiation therapy was a positive predictor of eventual tumor control [11], whereas others have found that a more protracted response was a better prognostic factor [7]. Thus, the use of volumetric-based measurements especially during radiation treatment is unclear at this time, although the combined use of CT and endoscopic evaluation has been suggested to predict for a good response to chemotherapy and a greater likelihood of organ preservation in head and neck cancer of the larynx, hypopharynx, and oropharynx [12–16].

Functional imaging–based assessments have also been assessed recently. Positron emission tomography using ^{18}F-fluoro-deoxy-glucose (FDG-PET) has been proven to predict for response to chemoradiotherapy in patients with head and neck cancer when measured several months after treatment [17,18]. In addition, a negative FDG-PET scan has been demonstrated to predict response in cervical lymph node metastases of head and neck cancer, therefore eliminating the need for post treatment neck dissection in patients who achieve a CR by FDG-PET [17]. However, currently, there is limited evidence for the use of PET during radiotherapy, and indeed, there is concern that acute inflammation caused by radiation of mucosal tissues could lead to false-positive determinations using FDG-PET [19]. Dynamic contrast-enhanced MRI [20] or other perfusion-based techniques [21] are alternative imaging modalities, which have been evaluated as early markers of response in head and neck cancer.

An imaging approach that is rapidly gaining interest for the detection of cancer treatment response is diffusion MRI [22] (Figure 1). Diffusion MRI is sensitive to the subcellular motion of water in biologic tissues and has been demonstrated to be effective both in diagnosing head and neck cancers [23] and in detecting relapses many months after the completion of radiation therapy [24]. However, the use of diffusion MRI during treatment of head and neck cancer has not been appropriately evaluated. Diffusion MRI early in a course of treatment would allow for the detection of alterations in tumor cell membrane integrity (i.e., microenvironment) after a therapeutic intervention using the Brownian motion of water (e.g., water diffusion) as a surrogate. This is accomplished based on the use of diffusion MRI pulse sequences allowing for collection of multislice image data sets wherein the magnetic resonance signal intensity is dependent on the mobility of the water molecules within the tissue [25]. At the start of treatment, tumors are anticipated to be densely cellular with a diffusion histogram reflective of this (Figure 1, *top panel*). Shortly after initiation of an effective treatment, there is initial breakdown of cellular membranes, which is detectable as a shift in the diffusion histogram to the right to more closely approximate an environment with increased water mobility, and this increase in water diffusion precedes overt volumetric changes in tumor size (Figure 1, *middle panel*). Finally, after the completion of an effective treatment, frank tumor death (necrotic or apoptotic) leads to further breakdown of cells and broadening of the diffusion histogram and often with a coincident decrease in tumor volume (Figure 1, *bottom panel*).

The initial application of diffusion MRI for the detection of tumor treatment response was reported using a rodent glioma model [26]. Further validation studies have expanded significantly on these initial results using a variety of tumor models and therapeutic agents [27–31]. Overall, these studies have shown that diffusion MRI can serve as a sensitive imaging biomarker for the detection of early cellular changes in treated tumors, which precede macroscopic volumetric response. Moreover, diffusion MRI measurements can be used to identify spatially distinct regional responses to therapy in tumors [31–35]. Translation of diffusion MRI into brain tumor clinical trials has been accomplished [33,34,36] where changes in diffusion measures have recently been shown to be strongly correlated both with overall clinical response based on the World Health Organization response criteria [34,36] and with overall survival [33]. In addition, preliminary data would also support diffusion MRI as an early response metric to combined chemoradiotherapy in head and neck cancer [37,38]. Thus, diffusion MRI is emerging as an important predictive biomarker for early stratification of tumor response.

The purpose of the current study was to evaluate whether diffusion MRI could be extended to assess treatment effects in SCCHN. The murine SCCVII squamous tumor model was used with cells genetically engineered to express a therapeutic transgene [yeast cytosine deaminase (*yCD*)], which, when exposed to a prodrug, 5-fluorocytosine (5FC), generates high concentrations of the chemotherapeutic agent 5-fluorouracil (5FU) locally within the tumor [39]. Treatment effects on diffusion were evaluated after treatment with radiation and radiochemotherapy and revealed that SCCVII tumor diffusion changes were correlated with treatment outcome measures (tumor burden and survival) better than conventional radiographic response, suggesting that further translational clinical studies are warranted.

Materials and Methods

Orthotopic Tumor Implantation

All of the animal work was carried out in the animal facility at the University of Michigan in accordance with federal, local, and institutional guidelines. Briefly, a *yCD*-expressing murine squamous SCCVII stable cell line was established by retroviral infection and limiting dilution in 96-well plates as previously reported [39]. These SCCVII cells (grown in medium culture) were trypsinized, washed

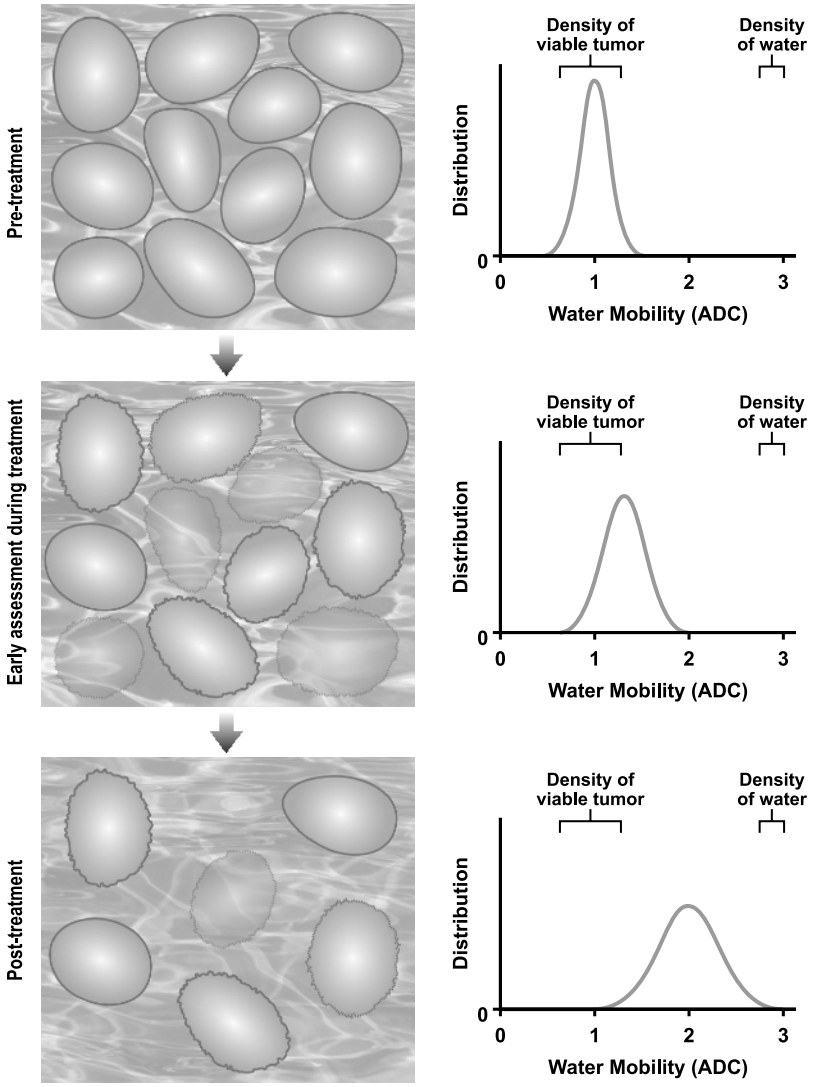

Figure 1. Schematic representation of diffusion MRI measured response to therapy. Changes in tumor cellularity (left) and increased molecular water mobility measured as the ADC (right) as a tumor responds to treatment (top to bottom). For a tumor responding to therapy, an increase in extracellular space/membrane permeability would be anticipated to increase both water mobility and ADC.

in phosphate-buffered saline (PBS), counted, and resuspended at a concentration of 4×10^8 cells/ml in PBS. Fifty microliters of this cell solution was injected into the submental compartment of C3H mice (6-8 weeks; Charles River Laboratories, Wilmington, MA) along the midline, using an external approach [39–41]. Mice were weighed every 2 to 3 days and were euthanized if they exceeded a body weight loss of >25%. For all studies, animals were anesthetized with an air/isoflurane (1.25%) mixture.

Chemotherapy and Radiation Treatment

Twenty-four animals with SCCVII tumors were entered into the study. Treatment was delivered as previously described [41]. When *in vivo* tumor volumes reached 15 to 20 μl, animals were divided into four groups. Group 1 was designated as the control group that received 0.1 ml of drug vehicle (10% ethanol in PBS daily by i.p. injection; $n = 6$). Groups 2, 3, and 4 received 5FC ($n = 6$), radiation ($n = 6$), and 5FC plus radiation ($n = 6$), respectively. All 5FC treatments (500 mg/kg daily) were administered by a single i.p. injection on days 0 to 4. Groups 3 and 4 animals received five doses of ionizing radiation at 4 Gy/day delivered on days 0 to 4. T2-weighted and diffusion MRI was performed every other day ($n = 3$ per imaging group) to measure volumetric and tumor water diffusion changes, respectively. Animal survival data were also obtained for all animals.

Magnetic Resonance Imaging

Tumors were imaged over a 3 week time frame using a Varian Unity Inova MRI system (Varian Instruments, Fremont, CA) equipped with a 7-T, 18.3-cm horizontal bore magnet (Oxford Instruments, Oxford, UK). During all MRI procedures, animals were anesthetized using 1.25% isoflurane, and body temperature was maintained at 37°C using a heated water recirculating pad. For anatomical imaging, a "fast spin-echo multislice" MRI sequence (TR/TE = 4000/60 milliseconds, number of transitients = 4, number of echoes = 8, FOV = 30 × 30 mm, image matrix = 128 × 128, slice thickness = 1 mm) was used to collect 13 contiguous T2-weighted images.

Maps of tumor apparent diffusion coefficient (ADC) values were acquired using a recently described method [31]. Briefly, a trace diffusion-weighted multislice spin-echo sequence (with motion compensation

and a navigator echo) was used to acquire 13 slices with two different diffusion weightings (b_1 = 100 and b_2 = 1248 sec/mm^2). The image slice thickness was 1 mm, image matrix was 128 × 128 (zero filled to 256), field of view was 30 × 30 mm, and echo time was 60 milliseconds. The images acquired with b_1 were essentially T2-weighted images, and these were used to segment the tumor from nontumor tissue for volumetric analysis using an "in-house" region drawing tool developed in Matlab.

Statistical Analysis

A 2-tailed *t* test was used to compare volume and diffusion data between groups. For comparison of animal overall survival, a log rank test was performed. Statistical analysis was performed using MedCalc (MedCalc, Version 9.5.1, Mariakerke, Belgium) with $P < .05$ considered to be statistically significant.

Results

Development of Orthotopic Model of Concurrent Chemoradiotherapy

In this study, we used an orthotopic model of SCCHN, which was previously demonstrated to mimic the locally invasive nature of this disease [39–41]. Murine squamous cells (SCCVII) were injected submentally forming a locally infiltrative tumor with near 100% tumor take. Tumors were allowed to grow sufficiently to have measurable dimensions for MRI-based imaging (15-20 µl at 3 days after implantation; Figure 2). As previously reported, we found that radiation therapy alone (4 Gy × 5 daily fractions) had limited efficacy in this model given the rapid growth of the tumor and the constraints on radiation dose caused by adjacent normal mucosa [41]. Combined chemoradiotherapy in this model using conventional agents (cisplatin, 5FU, or gemcitabine) was also found to be problematic owing to the abrupt and abundant mucositis and corresponding weight loss that developed. We initially tested the above three chemoradiotherapy regimens in non–tumor-bearing mice with radiation administered to the oral mucosa, and median weight loss within the first 2 weeks was >25% with a significant number of animals requiring euthanasia secondary to treatment toxicity (data not shown). We thus engendered to find an alternative model for concurrent chemoradiotherapy, which would limit the acute mucosal reactions and morbidity and allow evaluation of early MRI markers of treatment response [39,41].

Previously, we have reported on the use of genetically modified cells stably expressing either bacterial [41] or yeast cytosine deaminase [39], which allow the local conversion of 5FC, a nontoxic prodrug, to 5FU, a commonly used chemotherapeutic and radiosensitizing agent. Use of this gene therapy strategy was tolerable in this orthotopic model either alone or when combined with fractionated external beam radiotherapy [39,41]. Therefore, to serve as a model for concurrent chemoradiotherapy, orthotopic tumors that expressed yeast cytosine deaminase were developed, which were then treated with systemic 5FC either with or without fractionated external beam radiotherapy. After implantation, tumors expressing *yCD* readily grew within the submental compartment with a tumor-doubling time (4.1 ± 0.8 days) that was indistinguishable from wild type SCCVII cells [40,41] ($P > .1$; Figures 2*A* and 3).

Concurrent Chemoradiotherapy Does Not Increase the Rate of Response in Head and Neck Tumors

To test the use of radiation therapy either alone or when combined with systemically administered 5FC in *yCD*-expressing tumors in the submental compartment, animals were separated into four treatment groups. Control animals received a daily i.p. injection of carrier solution for 5 days. Radiation-treated animals were treated with 4 Gy daily for five consecutive days. Chemotherapy-treated animals received five consecutive daily i.p. injections of 5FC (500 mg/kg). Finally, combined modality–treated animals received both daily 5FC for 5 days along with five fractions of radiation (4 Gy each) delivered

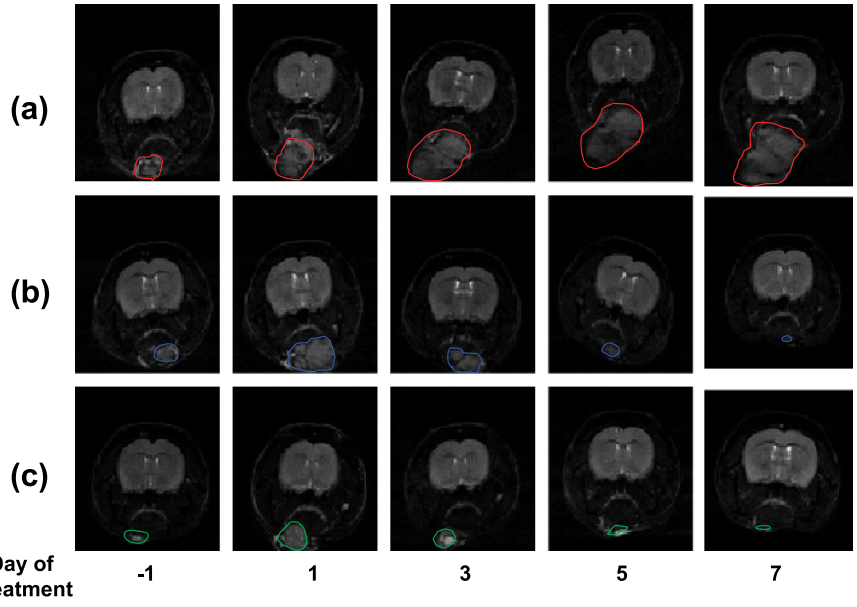

Figure 2. Submental tumor growth. Sequential T2-weighted MRI images of a slice through a control (A), a 5FC-treated (B), and a 5FC and radiation–treated (C) *yCD*-expressing SCCVII tumor. Images were acquired 1 day before therapy and 1, 3, 5, and 7 days after therapy. The submental tumors are indicated by the red, blue, and green regions of interest, respectively.

concurrent with chemotherapy treatment. A total of six animals were treated in each group for toxicity and survival analysis, and at the start of the study, three animals from each group were randomly selected for sequential imaging with MRI.

Figure 2 displays sequential representative T2-weighted MRI slices from one animal from each group, whereas Figure 3 displays the overall tumor growth curve. The maximum tumor diameter is depicted at each time point on the images, although all measures of response were based on volumetric analysis across all MRI slices. These diffusion-weighted images are essentially heavily T2-weighted with areas of increasing diffusion depicted as a higher intensity signal. As can be seen in Figure 2 *A*, control animals had tumors that grew rapidly after implantation with a locally invasive and exophytic tumor developing within the submental compartment. These tumors were also relatively solid with an ADC, which approximated that of surrounding muscle (Figure 2*A*); however, during the first week, as untreated tumors grew (Figure 3), they become more solid and cellular with a decrease in the ADC (Figure 4). Treatment with fractionated radiation therapy alone had only limited impact on tumor growth (Figure 3) that was not significantly different from control animals. In addition, the diffusion characteristics of these tumors approximated surrounding soft tissues with no significant increase in diffusion signal (Figure 4). In animals treated with systemic 5FC (Figure 2*B*), there was a marked arrest of tumor growth within 3 days after treatment, with a complete regression of tumor witnessed by day 7 of treatment; however, there was no significant increase in diffusion signal within the tumors during this period of tumor regression (Figure 2*B*). Finally, in animals treated with combination therapy (Figure 2*C*), there was also a significant regression of tumor leading to a CR by day 7 after treatment, which paralleled the 5FC-treated animals in the rate and extent of response (Figure 3). However, unlike the 5FC-treated animals, there was a substantial rise in the ADC of the submental tumors as witnessed by the greatly increased signal within the tumor (Figure 2*C*).

A comparison of the rate of tumor growth across all animals revealed a near constant growth of control tumors reaching a volume more than threefold larger than the starting size 9 days after the start of treatment (and 12 days after implantation; Figure 3, *open squares*). In animals treated with daily fractionated radiation, there was only limited growth delay that was not statistically significant when compared with control tumors (Figure 3, *closed squares*). In contrast, treatment with daily 5FC (Figure 3, *open circles*) resulted in rapid tumor shrinkage such that no measurable tumor was identifiable as early as 9 days after the start of treatment. Finally, in animals treated with combination therapy (Figure 3, *closed circles*), there was also an abrupt shrinkage of tumor resulting in a radiographic CR by 9 days after treatment. The rates of tumor regression in 5FC- or combination-treated animals were both statistically different from the control– and radiation-treated groups from day 3 of treatment onward (all P values in pairwise comparison <.04). In contrast, there was no significant difference between the growth rates of control- and radiation-treated animals ($P > .1$) or between the 5FC or combination therapy groups ($P > .1$).

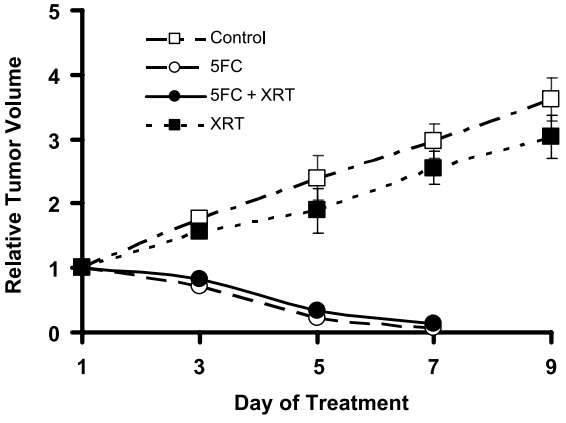

Figure 3. *In vivo* orthotopic tumor growth. Relative tumor volumes (±SEM; as measured on T2-weighted MRI) as a function of time after therapy for control-, 5FC-, 5FC and radiation–, and radiation-treated *yCD*-expressing SCCVII tumors.

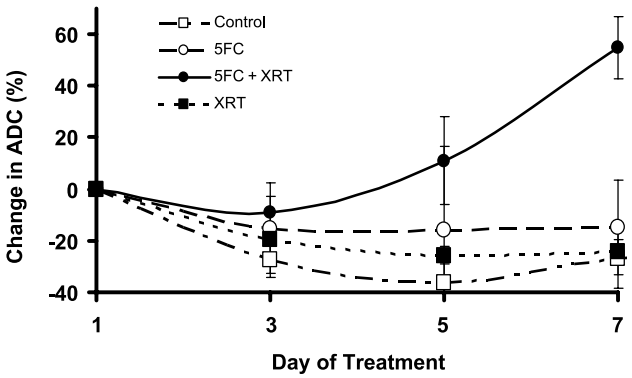

Figure 4. *In vivo* orthotopic tumor ADC changes. Mean ADC values (±SEM; as measured diffusion-weighted MRI) as a function of time after therapy for control-, 5FC-, 5FC and radiation–, and radiation-treated *yCD*-expressing SCCVII tumors.

Diffusion MRI Predicts Enhanced Response to Combined Therapy

Unlike the volumetric measures, which could not distinguish between the two treatment groups involving chemotherapy, when the mean ADC in the tumor masses were calculated, it was apparent that the combination therapy animals were exhibiting a much more abrupt rise in ADC (Figure 4, *closed circles*), which was different from the other three groups by 5 days after treatment and this difference continued to increase. The area under the curve of the change in the ADC as a function of time for combination therapy was statistically different from all other treatment groups ($P < .03$, $P < .04$, and $P < .05$, respectively, when compared with control-, radiation-, and 5FC-treated groups). In contrast, there was no significant difference between the remaining treatment groups; although there was a trend toward a greater area under the curve for 5FC-treated animals when compared with radiation-treated or control animals ($P < .08$).

Combined Modality Therapy Led to Enhanced Tumor Control

Overall tumor control and animal survival were evaluated, and there was no significant difference in tumor control or median survival between control- and radiation-treated groups (Figure 5). There was a trend toward a slightly increased median survival time in animals treated with radiation when compared with controls (33 *vs* 28 days); however, this difference did not achieve statistical significance ($P > .1$). In contrast, in animals treated with daily 5FC, there

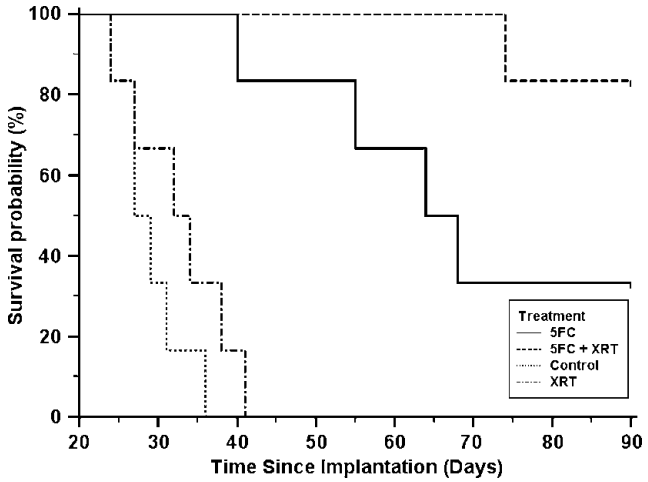

Figure 5. Overall animal survival with *in vivo* orthotopic tumors. Relative survival probability as a function of time after implantation for control-, 5FC-, 5FC and radiation–, and radiation-treated *yCD*-expressing SCCVII tumors.

was improved tumor control, with two of six animals free of tumor 90 days after tumor implantation and a median survival of 66 days that was statistically different from both control- and radiation-treated animals ($P < .0006$ for each). Finally, in the combination therapy group of animals, a greatly enhanced tumor control was observed when compared to all other groups, with five of six animals free of tumor 90 days after implantation and the median survival time that was not reached. Survival in the combination treatment group was statistically improved when compared not only to control- or radiation-treated animals ($P < .0006$ for each) but also to those animals treated with 5FC only ($P < .05$). At the time of death of all animals in each of these four groups, there was a grossly identifiable tumor within the submental compartment at postmortem analysis. In contrast, at the end of the experiment (90 days after implantation), there was no radiographically or grossly identifiable disease in any of the seven animals left alive in the 5FC or combination therapy groups.

Discussion

Treatment of head and neck cancer once the province of surgical resection alone is becoming more and more a multimodality disease [2,3]. However, the best way to integrate these different modalities is still not completely clear. Each of the commonly used treatments (surgery, radiation therapy, and chemotherapy) has its own unique benefits and toxicities. The goal of multimodality therapy is to judiciously use each of these treatments in a manner that maximizes benefit while limiting toxicity. The goal of early assessments of treatment response would be to allow an early and accurate evaluation of treatment efficacy, which would enable treatments to be tailored between individual patients instead of simply applying a treatment based on population norms or historical treatment information.

Standard volumetric-based assessments of treatment response in patients with head and neck cancer after induction chemotherapy have enabled selection of patients who are likely to benefit from subsequent radiotherapy or chemoradiotherapy [12–14,16]. However, these regimens have often entailed as many as three cycles of chemotherapy delivered for 9 or more weeks, which greatly increased the time and morbidity of treatment without providing any improvement in patient survival [12–14]. The use of volumetric measures during or shortly after radiotherapy has been difficult and has been found to only poorly correlate with eventual pathologic tumor control. In contrast, response as assessed by CT scan or PET many weeks to months after radiotherapy does have prognostic information regarding tumor control but is hampered by the long time after treatment to assess the response and would not allow adaptive radiotherapy based on intratreatment assessment of response.

In the current study, we tested a novel imaging technique to compare the differences in diffusion-weighted imaging within a tumor mass in response to treatment as a metric for eventual tumor control. The model system used incorporated a rapidly growing SCCHN line that is only minimally responsive to radiotherapy as revealed by both standard MRI [41] and diffusion MRI. Either chemotherapy, using a novel enzyme/prodrug gene therapy system, or the combination of chemotherapy and radiotherapy gave excellent response with complete regression of tumor observed in all animals. Despite complete radiographic response to single-agent chemotherapy, four of six animals eventually recurred with large submental tumors. Supporting our earlier work with this system [39,41], the combination of radiotherapy and chemotherapy did result in increased tumor control and enhanced animal survival compared with either chemotherapy or radiotherapy alone with five of six animals alive and free of disease 90 days after tumor implantation.

Diffusion MRI has previously been demonstrated to correlate with cellular density in rodent models of glioma and breast cancer [42–44]. In addition, changes in diffusion-weighted imaging have been proposed as a marker for early treatment response in both animal models of glioma [35,43] and in patients receiving chemotherapy or radiotherapy for primary brain tumors [33,34,36,45,46]. In patients with primary central nervous system malignancies, the combination of diffusion-weighted imaging both before and 3 weeks after the start of treatment has been demonstrated to predict eventual radiographic response at 10 weeks with both high sensitivity and specificity [36]. In addition, in a subset of patients with high-grade malignant glioma, diffusion-weighted imaging obtained as early as 3 weeks after the start of a course of fractionated radiation therapy predicted not only radiographic response but also time to progression and overall survival [33,34]. In our studies of glioma, we have found that a regional evaluation of diffusion response was more predictive of survival than simple measurements in the increase in overall average ADC [33–36]; however, in this animal model, given the very small size of tumors and their rapid growth rate, this regional evaluation was not feasible. Therefore, it is possible that, with further technologic application, this regional evaluation of diffusion response will be even more predictive of later clinical outcome.

One further potential advantage demonstrated in this study, which needs to be explored, is the fact that, even with CR to therapy, 5 of 12 animals eventually recurred (4/6 in the 5FC group and 1/6 in the 5FC + radiation group). In contrast, the much greater rise in ADC observed in the combined modality group only 3 days into treatment correlated with a significantly greater tumor control. We previously observed this phenomenon in a rodent glioma tumor model as well where radiographic CR to treatment was poorly correlated with tumor control, whereas a radiographic CR in the setting of a threefold rise in tumor ADC predicted for long-term tumor control [47]. The lack of a CR to chemotherapy correlating with significant clinical advantage would also be supported by the extensive experience with

induction chemotherapy in head and neck cancer where as many as 30% to 40% of patients could be rendered radiographically free of disease before radiotherapy with only a very modest improvement in survival [4]. In contrast, a more intensive therapy with concurrent chemotherapy and radiation therapy has been associated with a significantly greater survival advantage [4].

Thus, in preclinical and clinical evaluation of head and neck cancer, a rapid CR to chemotherapy did not predict for ultimate tumor control. However, the preclinical data presented here for diffusion MRI suggest that this technique may be able to differentiate between those radiographic responses that are more likely to be durable. Initial experience with diffusion MRI in head and neck cancer supports this technique as technically achievable in patients with head and neck cancer being treated with concurrent chemoradiotherapy. In two pilot studies, significant increases in tumor ADC were observed as early as 1 [38] to 2 weeks [37] into chemoradiotherapy that seem to predict subsequent radiographic response. It remains to be seen if further evaluation of diffusion MRI as an early biomarker of response will enable patient-specific tailoring of chemotherapy and radiation therapy in patients with head and neck cancer to maintain tumor control while decreasing the overall toxicity of treatment and increasing patient quality of life.

References

[1] Jemal A, Siegel R, Ward E, Hao Y, Xu J, Murray T, and Thun MJ (2008). Cancer statistics, 2008. *CA Cancer J Clin* **58** (2), 71–96.

[2] Salama JK, Seiwert TY, and Vokes EE (2007). Chemoradiotherapy for locally advanced head and neck cancer. *J Clin Oncol* **25** (26), 4118–4126.

[3] Forastiere AA, Ang K, Brizel D, Brockstein BE, Dunphy F, Eisele DW, Goepfert H, Hicks WL Jr, Kies MS, Lydiatt WM, et al. (2005). Head and neck cancers. *J Natl Compr Canc Netw* **3** (3), 316–391.

[4] Bourhis J, Le Maitre A, Baujat B, Audry H, and Pignon JP (2007). Individual patients' data meta-analyses in head and neck cancer. *Curr Opin Oncol* **19** (3), 188–194.

[5] Feng M and Eisbruch A (2007). Future issues in highly conformal radiotherapy for head and neck cancer. *J Clin Oncol* **25** (8), 1009–1013.

[6] Klug C, Keszthelyi D, Ploder O, Sulzbacher I, Voracek M, Wagner A, Millesi W, Kornek G, Kainberger F, Kermer C, et al. (2004). Neoadjuvant radiochemotherapy of oral cavity and oropharyngeal cancer: evaluation of tumor response by CT differs from histopathologic response assessment in a significant fraction of patients. *Head Neck* **26** (3), 224–231.

[7] Denys D, Kumar P, Wong FS, Newman LA, and Robbins KT (1997). The predictive value of tumor regression rates during chemoradiation therapy in patients with advanced head and neck squamous cell carcinoma. *Am J Surg* **174** (5), 561–564.

[8] Ojiri H, Mendenhall WM, and Mancuso AA (2002). CT findings at the primary site of oropharyngeal squamous cell carcinoma within 6-8 weeks after definitive radiotherapy as predictors of primary site control. *Int J Radiat Oncol Biol Phys* **52** (3), 748–754.

[9] Ojiri H, Mendenhall WM, Stringer SP, Johnson PL, and Mancuso AA (2002). Post-RT CT results as a predictive model for the necessity of planned post-RT neck dissection in patients with cervical metastatic disease from squamous cell carcinoma. *Int J Radiat Oncol Biol Phys* **52** (2), 420–428.

[10] Ma X, Lu JJ, Loh KS, Shakespeare TP, Thiagarajan A, Goh BC, and Tan KS (2006). Role of computed tomography imaging in predicting response of nasopharyngeal carcinoma to definitive radiation therapy. *Laryngoscope* **116** (12), 2162–2165.

[11] Jaulerry C, Dubray B, Brunin F, Rodriguez J, Point D, Blaszka B, Asselain B, Mosseri V, Brugere J, and Cosset JM (1995). Prognostic value of tumor regression during radiotherapy for head and neck cancer: a prospective study. *Int J Radiat Oncol Biol Phys* **33** (2), 271–279.

[12] Spaulding MB, Fischer SG, and Wolf GT (1994). Tumor response, toxicity, and survival after neoadjuvant organ-preserving chemotherapy for advanced laryngeal carcinoma. The Department of Veterans Affairs Cooperative Laryngeal Cancer Study Group. *J Clin Oncol* **12** (8), 1592–1599.

[13] Urba SG, Wolf GT, Bradford CR, Thornton AF, Eisbruch A, Terrell JE, Carpenter V, Miller T, Tang G, and Strawderman M (2000). Neoadjuvant therapy for organ preservation in head and neck cancer. *Laryngoscope* **110** (12), 2074–2080.

[14] Urba SG, Moon J, Giri PG, Adelstein DJ, Hanna E, Yoo GH, Leblanc M, Ensley JF, and Schuller DE (2005). Organ preservation for advanced resectable cancer of the base of tongue and hypopharynx: a Southwest Oncology Group Trial. *J Clin Oncol* **23** (1), 88–95.

[15] Urba S, Wolf G, Eisbruch A, Worden F, Lee J, Bradford C, Teknos T, Chepeha D, Prince M, Hogikyan N, et al. (2006). Single-cycle induction chemotherapy selects patients with advanced laryngeal cancer for combined chemoradiation: a new treatment paradigm. *J Clin Oncol* **24** (4), 593–598.

[16] Worden FP, Kumar B, Lee JS, Wolf GT, Cordell KG, Taylor JM, Urba SG, Eisbruch A, Teknos TN, Chepeha DB, et al. (2008). Chemoselection as a strategy for organ preservation in advanced oropharynx cancer: response and survival positively associated with HPV16 copy number. *J Clin Oncol* **26** (19), 3138–3146.

[17] Yao M, Smith RB, Graham MM, Hoffman HT, Tan H, Funk GF, Graham SM, Chang K, Dornfeld KJ, Menda Y, et al. (2005). The role of FDG PET in management of neck metastasis from head-and-neck cancer after definitive radiation treatment. *Int J Radiat Oncol Biol Phys* **63** (4), 991–999.

[18] McCollum AD, Burrell SC, Haddad RI, Norris CM, Tishler RB, Case MA, Posner MR, and Van den Abbeele AD (2004). Positron emission tomography with ^{18}F-fluorodeoxyglucose to predict pathologic response after induction chemotherapy and definitive chemoradiotherapy in head and neck cancer. *Head Neck* **26** (10), 890–896.

[19] Mukherji SK and Wolf GT (2003). Evaluation of head and neck squamous cell carcinoma after treatment. *AJNR Am J Neuroradiol* **24** (9), 1743–1746.

[20] Tomura N, Omachi K, Sakuma I, Takahashi S, Izumi J, Watanabe O, Watarai J, and Sageshima M (2005). Dynamic contrast-enhanced magnetic resonance imaging in radiotherapeutic efficacy in the head and neck tumors. *Am J Otolaryngol* **26** (3), 163–167.

[21] Gandhi D, Chepeha DB, Miller T, Carlos RC, Bradford CR, Karamchandani R, Worden F, Eisbruch A, Teknos TN, Wolf GT, et al. (2006). Correlation between initial and early follow-up CT perfusion parameters with endoscopic tumor response in patients with advanced squamous cell carcinomas of the oropharynx treated with organ-preservation therapy. *AJNR Am J Neuroradiol* **27** (1), 101–106.

[22] Hamstra DA, Rehemtulla A, and Ross BD (2007). Diffusion magnetic resonance imaging: a biomarker for treatment response in oncology. *J Clin Oncol* **25** (26), 4104–4109.

[23] Wang J, Takashima S, Takayama F, Kawakami S, Saito A, Matsushita T, Momose M, and Ishiyama T (2001). Head and neck lesions: characterization with diffusion-weighted echo-planar MR imaging. *Radiology* **220** (3), 621–630.

[24] Vandecaveye V, De Keyzer F, Nuyts S, Deraedt K, Dirix P, Hamaekers P, Vander Poorten V, Delaere P, and Hermans R (2007). Detection of head and neck squamous cell carcinoma with diffusion weighted MRI after (chemo)radiotherapy: correlation between radiologic and histopathologic findings. *Int J Radiat Oncol Biol Phys* **67** (4), 960–971.

[25] Le Bihan D, Breton E, Lallemand D, Grenier P, Cabanis E, and Laval-Jeantet M (1986). MR imaging of intravoxel incoherent motions: application to diffusion and perfusion in neurologic disorders. *Radiology* **161** (2), 401–407.

[26] Ross BD, Chenevert TL, Kim B, and Ben-Joseph O (1994). Magnetic resonance imaging and spectroscopy: application to experimental neuro-oncology. *Q Magn Reson Biol Med* **1**, 89–106.

[27] Chenevert TL, McKeever PE, and Ross BD (1997). Monitoring early response of experimental brain tumors to therapy using diffusion magnetic resonance imaging. *Clin Cancer Res* **3** (9), 1457–1466.

[28] Brunberg JA, Chenevert TL, McKeever PE, Ross DA, Junck LR, Muraszko KM, Dauser R, Pipe JG, and Betley AT (1995). *In vivo* MR determination of water diffusion coefficients and diffusion anisotropy: correlation with structural alteration in gliomas of the cerebral hemispheres. *AJNR Am J Neuroradiol* **16** (2), 361–371.

[29] Ross BD, Ben-Joseph O, and Chenevert TL (1997). *In vivo* magnetic resonance imaging and spectroscopy. Application to brain tumors. In H Bachelard (Ed.) *Magnetic Resonance Spectroscopy and Imaging in Neurochemistry.* New York, NY: Plenum Press, pp. 145–178.

[30] Poptani H, Puumalainen AM, Grohn OH, Loimas S, Kainulainen R, Yla-Herttuala S, and Kauppinen RA (1998). Monitoring thymidine kinase and ganciclovir-induced changes in rat malignant glioma *in vivo* by nuclear magnetic resonance imaging. *Cancer Gene Ther* **5** (2), 101–109.

[31] Moffat BA, Hall DE, Stojanovska J, McConville PJ, Moody JB, Chenevert TL, Rehemtulla A, and Ross BD (2004). Diffusion imaging for evaluation of tumor therapies in preclinical animal models. *Magma* **17** (3–6), 249–259.

[32] Hall DE, Moffat BA, Stojanovska J, Johnson TD, Li Z, Hamstra DA, Rehemtulla A, Chenevert TL, Carter J, Pietronigro D, et al. (2004). Therapeutic efficacy of DTI-015 using diffusion magnetic resonance imaging as an early surrogate marker. *Clin Cancer Res* **10** (23), 7852–7859.

[33] Hamstra DA, Galban CJ, Meyer CR, Johnson TD, Sundgren PC, Tsien C, Lawrence TS, Junck L, Ross DJ, Rehemtulla A, et al. (2008). Functional diffusion map as an early imaging biomarker for high-grade glioma: correlation with conventional radiologic response and overall survival. *J Clin Oncol* **26** (20), 3387–3394.

[34] Hamstra DA, Chenevert TL, Moffat BA, Johnson TD, Meyer CR, Mukherji SK, Quint DJ, Gebarski SS, Fan X, Tsien CI, et al. (2005). Evaluation of the functional diffusion map as an early biomarker of time-to-progression and overall survival in high-grade glioma. *Proc Natl Acad Sci USA* **102** (46), 16759–16764.

[35] Moffat BA, Chenevert TL, Meyer CR, McKeever PE, Hall DE, Hoff BA, Johnson TD, Rehemtulla A, and Ross BD (2006). The functional diffusion map: an imaging biomarker for the early prediction of cancer treatment outcome. *Neoplasia* **8** (4), 259–267.

[36] Moffat BA, Chenevert TL, Lawrence TS, Meyer CR, Johnson TD, Dong Q, Tsien C, Mukherji S, Quint DJ, Gebarski SS, et al. (2005). Functional diffusion map: a noninvasive MRI biomarker for early stratification of clinical brain tumor response. *Proc Natl Acad Sci USA* **102** (15), 5524–5529.

[37] Chenevert TL, Mukerji S, Eisbruch A, Meyer CR, Hamstra DA, Kim HS, Ross BD, Rehemtulla A, and Moffat BA (2006). Functional diffusion mapping as an early imaging biomarker for therapeutic efficacy in head and neck cancer. Intl Soc Mag Reson Med 14th Annual Meeting; 2006; Seattle, WA.

[38] Kim S, Loevner LA, Quon H, Sherman EJ, Weinstein GS, and Poptani H (2008). Monitoring response to chemoradiotherapy of squamous cell carcinoma of the head and neck using diffusion weighted MRI. Intl Soc Mag Reson Med 16th Annual Meeting; May 3–9, 2008; Toronto, p. 3465.

[39] Hamstra DA, Rice DJ, Fahmy S, Ross BD, and Rehemtulla A (1999). Enzyme/prodrug therapy for head and neck cancer using a catalytically superior cytosine deaminase. *Hum Gene Ther* **10** (12), 1993–2003.

[40] Dinesman A, Haughey B, Gates GA, Aufdemorte T, and Von Hoff DD (1990). Development of a new *in vivo* model for head and neck cancer. *Otolaryngol Head Neck Surg* **103** (5 (Pt 1)), 766–774.

[41] Hamstra DA, Rice DJ, Pu A, Oyedijo D, Ross BD, and Rehemtulla A (1999). Combined radiation and enzyme/prodrug treatment for head and neck cancer in an orthotopic animal model. *Radiat Res* **152** (5), 499–507.

[42] Galons JP, Altbach MI, Paine-Murrieta GD, Taylor CW, and Gillies RJ (1999). Early increases in breast tumor xenograft water mobility in response to paclitaxel therapy detected by non-invasive diffusion magnetic resonance imaging. *Neoplasia* **1** (2), 113–117.

[43] Chenevert TL, Stegman LD, Taylor JM, Robertson PL, Greenberg HS, Rehemtulla A, and Ross BD (2000). Diffusion magnetic resonance imaging: an early surrogate marker of therapeutic efficacy in brain tumors. *J Natl Cancer Inst* **92** (24), 2029–2036.

[44] Chinnaiyan AM, Prasad U, Shankar S, Hamstra DA, Shanaiah M, Chenevert TL, Ross BD, and Rehemtulla A (2000). Combined effect of tumor necrosis factor–related apoptosis-inducing ligand and ionizing radiation in breast cancer therapy. *Proc Natl Acad Sci USA* **97** (4), 1754–1759.

[45] Mardor Y, Pfeffer R, Spiegelmann R, Roth Y, Maier SE, Nissim O, Berger R, Glicksman A, Baram J, Orenstein A, et al. (2003). Early detection of response to radiation therapy in patients with brain malignancies using conventional and high *b*-value diffusion-weighted magnetic resonance imaging. *J Clin Oncol* **21** (6), 1094–1100.

[46] Mardor Y, Roth Y, Lidar Z, Jonas T, Pfeffer R, Maier SE, Faibel M, Nass D, Hadani M, Orenstein A, et al. (2001). Monitoring response to convection-enhanced taxol delivery in brain tumor patients using diffusion-weighted magnetic resonance imaging. *Cancer Res* **61** (13), 4971–4973.

[47] Hamstra DA, Lee KC, Tychewicz JM, Schepkin VD, Moffat BA, Chen M, Dornfeld KJ, Lawrence TS, Chenevert TL, Ross BD, et al. (2004). The use of ^{19}F spectroscopy and diffusion-weighted MRI to evaluate differences in gene-dependent enzyme prodrug therapies. *Mol Ther* **10** (5), 916–928.